

## A Hybrid Adaptation Strategy for Repetitive Control of an Uncertain-Delay Lagrangian System

Andrea Tilli \* Elena Ruggiano \* Christian Conficoni \*  
Alessandro Bosso \*

\* *Department of Electrical, Electronic and Information Engineering,  
University of Bologna, Bologna, Italy (e-mail: {andrea.tilli,  
elena.ruggiano2,christian.conficoni3,alessandro.bosso3}@unibo.it).*

**Abstract:** In this work, we present a novel repetitive control (RC) strategy to achieve accurate position tracking of a 1-DOF Lagrangian system. Such controller is able to cope with model uncertainties and unknown transmission delays in the control architecture. The classic repetitive structure is augmented with an observer of the residual disturbance, to be compensated by means of the RC action. The repetitive unit is updated at hybrid instants, so that the disturbance observer is close to its steady-state before a new repetitive correction is applied. In addition, communication delay is also estimated by the proposed control structure. This way, practical asymptotic stability of the overall system can be achieved with a simple proportional correction of the RC, also under perturbations of the steady-state estimate due to model uncertainties. In light of the aforementioned properties, the proposed RC-based controller is shown to be an easy-to-tune, robust solution capable of improving the tracking performance for the given case of study.

Copyright © 2020 The Authors. This is an open access article under the CC BY-NC-ND license (<http://creativecommons.org/licenses/by-nc-nd/4.0>)

**Keywords:** Iterative and Repetitive learning control, Systems with time-delays, Motion Control Systems, Design methodologies, Mechatronic systems, Stability of hybrid systems

### 1. INTRODUCTION

In several engineering fields, such as industrial automation and robotics, the control problems come down to perform accurate periodic (with known period) motion profiles for complex nonlinear mechanisms. The standard technology adopted for these applications consists of commercial electric drives and a motion controller unit (usually a Programmable Logic Controller) (Gurocak, 2015). In this context, the controllers typically take the form of simple SISO cascade structures devoted to position, speed, and torque/current control, adopting linear feedback laws, combined with feedforward actions. The motion control unit is employed to generate reference profiles and it can provide, in some commercial platforms, the feedforward terms to the inner loops based on some knowledge about the controlled system dynamics. Tracking error measurements are also available to this unit, yet the communication protocol between drive and motion control device typically introduces significant and not fully known delays in both directions. This is detrimental for tracking performance, especially in presence of model uncertainties.

Natural frameworks to improve tracking of such systems are learning-type approaches, such as *Repetitive Control* (RC) and *Iterative Learning Control* (ILC). Roughly speaking, these methods exploit the internal model principle to generate a periodic signal, with known period, whose shape is updated exploiting information from previous iterations. This way, asymptotic reference tracking or disturbance rejection is achieved. We refer the reader to (Wang et al., 2009), (Ahn et al., 2007) (Longman, 2000) and references therein for a comprehensive overview.

Here, our objective is to endow the motion control with a RC structure, designed to achieve a very accurate tracking under the following conditions: (i) uncertain mechanical dynamics,

possibly affected by periodic torque disturbances, (ii) unknown transmission delay, (iii) no knowledge/exploitation of the drive controller. The main assumptions imposed to the inner controller are ultimate boundedness of the tracking error, and convergence to a periodic steady-state in absence of the RC action. In the related literature, a standard way to obtain robust learning control schemes is to introduce proper filtering (the so-called “q-filter”) in the repetitive signal generation structure (Królikowski and Baczyński, 2000), (Na et al., 2012). However, this perturbs the actual internal model effectiveness, degrading the tracking/rejection capability of the scheme typically for high frequency harmonics. Recently, robust solutions based on LMI design have been proposed in (Liu and Gao, 2010), (Yu et al., 2017), where however we find filtering or a nominal delay value (within known bounds). (Xu and Yan, 2006) achieves robustness against parametric uncertainties modifying the repetitive control law with a nonlinear damping term for a class of delay-free systems. (Watanabe and Yamada, 1990) and (Tan et al., 2009), instead, present some compensation methods for the case of known input delay.

The target of this work is to obtain robustness without resorting to filtering, i.e. preserving the RC internal model property w.r.t. any periodic shape. In addition, an adaptation mechanism is added to estimate and compensate the system communication delay. To this aim, the proposed method relies on an adaptation strategy of the RC, which is fed by the output of a model-based “equivalent disturbance” observer. This element is crucial to estimate the residual signal to be learned by the RC. Indeed, passivity and absolute stability arguments (Arimoto and Naniwa, 2000) can be used to prove stability, provided that the correction to the repetitive signal is sufficiently slow to let the estimated disturbance closely approach its steady state. This is possible also in case of no perfect steady-state reconstruction,

e.g. due to model mismatches. The overall system dynamics is analyzed employing the hybrid formalism (Goebel et al., 2012), where jumps are associated with the RC correction update and delay adaptation, while flows are given by the plant, the drive controller, the disturbance observer, and the periodic injection of the same RC action between updates. Note that the actual implementation of flows is given by discrete-time systems due to the digital nature of the computing devices. Still, the analysis is valid, as long as the sampling time of the discretized flows is small enough w.r.t. the intervals between jumps.

This paper is organized as follows. In Section 2 we present the model of the system to be controlled, a 1-DOF nonlinear mechanism, we define the controller architecture, and formulate the problem statement. Section 3 is devoted to introducing the proposed control solution, and analyzing its stability and robustness properties, while in Section 4 numerical simulation results are shown to validate the method. Finally, Section 5 provides some concluding remarks and future directions.

2. FRAMEWORK AND PROBLEM STATEMENT

In this Section, we introduce the considered mechanical system model, we define the motion control structure and the technological architecture, then we formulate the control problem.

2.1 Nonlinear 1-DOF Mechanism Model

We consider motion control of a 1-DOF Lagrangian system whose dynamics can be expressed by a differential equation of the form:

$$\dot{\theta} = \omega, \tag{1}$$

$$J(\theta)\dot{\omega} = -\frac{1}{2}\frac{\partial J}{\partial \theta}(\theta)\omega^2 - \frac{\partial U}{\partial \theta}(\theta) + \tau.$$

where  $\theta$  denotes the angular position of the prime mover connected to the electric drive,  $\omega$  is the corresponding angular speed, while  $\tau$  is the input torque provided by the motor<sup>1</sup>. Furthermore,  $J(\theta)$  is the reduced inertia and  $U(\theta)$  denotes the potential energy due to gravity. We can compactly rewrite the second row in (1) as:

$$\dot{\omega} = f(\theta, \omega) + g(\theta)\tau, \tag{2}$$

$$f(\theta, \omega) := \frac{1}{J(\theta)}\left(-\frac{1}{2}\frac{\partial J}{\partial \theta}(\theta)\omega^2 - \frac{\partial U}{\partial \theta}(\theta)\right), g(\theta) := \frac{1}{J(\theta)}.$$

The proposed method will be applied to a planar four-bar linkage, whose inertia and potential energy profiles, reported in Fig. 1, will be exploited to design the disturbance observer.

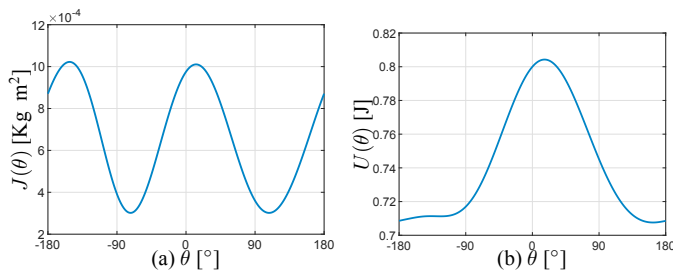


Fig. 1. Profiles of the inertia  $J(\theta)$  (a) and the potential energy  $U(\theta)$  (b) of the considered mechanism.

<sup>1</sup> A gearbox can be inserted between the drive and the mechanism, in this case  $\theta, \omega$  and  $\tau$  denote quantities downstream the gearbox.

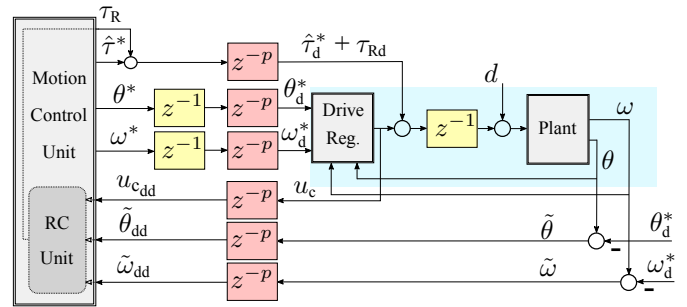


Fig. 2. Schematic representation of the control architecture of the considered system.

2.2 Motion Control Architecture

The standard motion control architecture is realized with two main units:

- an electric drive controller, given by a discrete-time regulator with sampling time  $T_s$ , which introduces a delay equal to  $T_s$  in the actuation due to the features of the real-time operating system;
- an orchestration unit, commonly referred to as the *motion controller*, which generates the reference trajectory for the drive controller and the corresponding feedforward terms.

For simplicity, we assume that the same sampling period of the drive is used in the motion controller. However, the ensuing analysis and results can be generalized to the common situations when they differ (often the motion unit sampling time is a multiple of the other). Here we will consider periodic profiles with known period  $T$  multiple of  $T_s$ . The general case can be handled by taking a larger repetition period, obtained as the least common multiple of  $T$  and  $T_s$ .

Besides generating references, the motion controller can provide feedforward terms to the drive, based on some knowledge of the system to be moved. Furthermore, the motion controller can also read the position and speed tracking errors measured at the drive side. The information is exchanged between the two control units by means of some communication protocol, which ensures determinism but also introduces a constant transmission delay.

The overall control structure is shown in Fig. 2, where  $(\cdot)_d$  indicates the delayed signal at the drive side, while  $(\cdot)_{dd}$  denotes the delayed information received by the motion controller from the drive. Note that for signals  $\theta_d^*, \omega_d^*$  there is an additional  $T_s$ -delay w.r.t.  $\hat{\tau}^*$  to account for the actuation delay.

For the considered benchmark, the motion controller and the drive sampling times have been set to  $T_s = 2 \times 10^{-4}$  s. Concerning the drive regulator, for the position loop, we considered a proportional feedback control with gain  $k_{p\theta} = 80$  Hz with a feedforward term  $\omega_d^*$  for the position loop. The velocity control loop is instead given by a PI controller, with proportional gain  $k_{p\omega} = 0.12$  Nm/(rad/s) and integral gain  $k_{i\omega} = 4.8 \times 10^{-4}$  Nm/rad combined with the aforementioned torque feedforward action coming from the motion controller.

2.3 Problem Statement and Control Objectives

We begin by formally stating the control problem. In the following, we distinguish the discrete-time controller signals (with sample time  $T_s$ ) from the continuous-time trajectories of the plant using  $kT_s$  and  $t$  as time arguments, respectively. This

choice is instrumental in simplifying the discussion (with some abuse of notation) when referring to  $T$ -periodic trajectories and the discrete-time samples of continuous-time signals.

From a technological perspective, we assume that the transmission delay is constant but fully unknown, i.e., it cannot be measured by suitable support infrastructure. From the control viewpoint, we suppose that the motion controller provides a feedforward torque  $\hat{\tau}^*$  (see Fig. 2), which approximates the ideal input  $\tau^*$  without perfect accuracy due to model uncertainties. In particular, consider a  $T$ -periodic reference trajectory  $\theta^*, \omega^*$  which can be perfectly tracked applying a piecewise constant torque command<sup>2</sup>. Therefore,  $\theta^*, \omega^*$  are related with  $\tau^*$  through a continuous-time trajectory, resulting from the application to (1) of the following input:

$$\bar{\tau}^*(t) = \tau^* \left( \left( \text{floor} \left( \frac{t}{T_s} \right) - p - 1 \right) T_s \right),$$

leading to the system:

$$\begin{aligned} \dot{\theta} &= \omega, & \theta(t_0) &= \bar{\theta}^*(t_0) \\ \dot{\omega} &= f(\theta, \omega) + g(\theta)\bar{\tau}^*, & \omega(t_0) &= \bar{\omega}^*(t_0) = \dot{\bar{\theta}}^*(t_0). \end{aligned} \quad (3)$$

It follows that the solution of system (3), indicated with  $\bar{\theta}^*(t), \bar{\omega}^*(t)$ , provides the relation with the discrete-time reference trajectory through  $\bar{\theta}^*(kT_s) = \theta_d^*(kT_s) = \theta^*((k-p-1)T_s)$ ,  $\bar{\omega}^*(kT_s) = \omega_d^*(kT_s) = \omega^*((k-p-1)T_s)$ . Consider a piecewise-constant torque signal  $\hat{\tau}^*$  of the form:

$$\hat{\tau}^*(t) = \hat{\tau}^* \left( \left( \text{floor} \left( \frac{t}{T_s} \right) - p - 1 \right) T_s \right),$$

and let  $\tilde{\tau} = \bar{\tau}^* - \hat{\tau}^*, \tilde{\theta} = \theta - \bar{\theta}^*, \tilde{\omega} = \omega - \bar{\omega}^*$ . Then, the error dynamics resulting from the application of  $\hat{\tau}^*$  is given as:

$$\begin{aligned} \dot{\tilde{\theta}} &= \tilde{\omega} \\ \dot{\tilde{\omega}} &= f(\bar{\theta}^* + \tilde{\theta}, \bar{\omega}^* + \tilde{\omega}) + g(\bar{\theta}^* + \tilde{\theta})(\bar{u} + \bar{\tau}^* - \tilde{\tau} + d) \\ &\quad - f(\bar{\theta}^*, \bar{\omega}^*) - g(\bar{\theta}^*)\bar{\tau}^*, \end{aligned} \quad (4)$$

with  $d$  a continuous-time disturbance (see Fig. 2) and  $\bar{u}$  a piecewise-constant input generated by the regulator in the drive controller, with output  $u_c$  and internal state  $z$ :

$$\begin{aligned} u_c(kT_s) &= h_1(\tilde{\theta}(kT_s), \tilde{\omega}(kT_s), z(kT_s)) \\ z((k+1)T_s) &= h_2(\tilde{\theta}(kT_s), \tilde{\omega}(kT_s), z(kT_s)) \\ \bar{u}(t) &= u_c \left( \left( \text{floor} \left( \frac{t}{T_s} \right) - 1 \right) T_s \right), \end{aligned} \quad (5)$$

As concerns the properties of the closed-loop system (4)-(5), we assume that an attractor satisfying  $(\tilde{\theta}, \tilde{\omega}) = 0$  is regionally asymptotically stable if  $d = 0, \tilde{\tau} = 0$ . Furthermore, we require that the system is ISS with restrictions w.r.t. the inputs  $d(\cdot) \in S_d, \tilde{\tau}(\cdot) \in S_\tau$ , where  $S_d$  and  $S_\tau$  are sets of  $T$ -periodic bounded signals.

*Remark 1.* The set  $S_d$ , is assumed to be composed by signals satisfying the following condition:  $\forall d(\cdot) \in S_d$  there exists a  $T$ -periodic signal  $d_d(\cdot)$  such that  $d_d(t) = d_d(\text{floor}(t/T_s)T_s)$  generates the same effect as  $d(\cdot)$  on the system, for all  $\theta(t_0), \omega(t_0)$  in the domain of attraction of the considered drive controller<sup>3</sup>.

<sup>2</sup> the definition of such profiles is in general a non-trivial task.

<sup>3</sup> This assumption is necessary to ensure the disturbance can be perfectly matched by the control action. In real applications such matching condition can be violated, as well as the ability to track the references. Nevertheless, small mismatches are expected to arise, which, thanks to the robustness of the proposed solution, should produce small residual steady-state tracking errors.

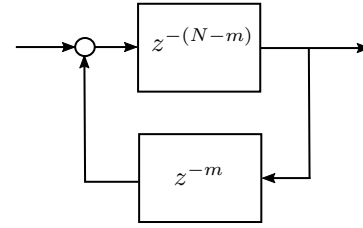


Fig. 3. Repetitive structure for delay compensation.

In the light of the previous considerations, we can formulate the objective pursued in this work as follows: introduce an additional control loop, acting on the left side of the system portrayed in Fig. 2, and generating a signal  $\tau_R$  to modify, in an additive manner, the signal  $\hat{\tau}^*$  sent to the drive (which otherwise would be just an inaccurate feedforward term based on mechanical model inversion), so that  $\tilde{\theta}, \tilde{\omega}$  asymptotically vanish, for all  $d(\cdot) \in S_d$  and all  $\tilde{\tau}(\cdot) \in S_\tau$ .

As mentioned, the solution to obtain this goal relies on a RC unit, which should also satisfy the ensuing properties:

- to deal with arbitrary  $T$ -periodic shapes of  $d$  and  $\tilde{\tau}$  (belonging to the respective sets  $S_d, S_\tau$ ), i.e., no filtering is required;
- to achieve robust stabilization, regardless of the drive controller model (as long as it provides ISS properties), and with mechanical model uncertainties (with mismatches bounded by the assumptions made on  $\tilde{\tau}$ );
- to have a simple and easy-to-tune structure, e.g., with a proportional correction law;
- to allow adaptation of the system delay, reconstructing the unknown constant value.

### 3. THE PROPOSED SOLUTION

Here we develop the proposed RC scheme and analyze its properties. Firstly, the case of known transmission delay is treated, then a suitable adaptation strategy is proposed to cope with the case when such information is lacking.

#### 3.1 Known delay case

Contrary to the more standard cases in which the RC unit is fed with the position tracking error, in our case, the RC unit takes as input the equivalent torque disturbance to be compensated to achieve perfect tracking. This way, exploiting the inherent convergence properties of the drive controller, an easy-to-tune RC unit is obtained, without any filters. According to the previous reasoning, the signal to reconstruct is  $d_T(kT_s) = -d_d(kT_s) + \tilde{\tau}(kT_s)$ ,  $k = 0, \dots, N-1$ , with  $N = T/T_s$ .

Let the transmission delay  $pT_s$  (see Fig. 2) be known. Any adopted reconstruction unit will be affected by the structural delay of the chain given by the communication infrastructure, the drive controller, and the plant itself. However, if such delay is known and given by  $mT_s$  ( $m \in \mathbb{N}$ ), it can be compensated introducing the repetitive scheme shown in Fig. 3. Regarding the structure and accuracy of the disturbance observer, the idea is to use only the mechanical dynamics, assuming the model to be uncertain. As a consequence, besides the aforementioned delay, any disturbance observer will be affected by inaccuracies both in its dynamic and steady-state behavior. The former can be particularly harmful for stability of the overall system. Indeed, even if the disturbance observer is expected to be stable

and convergent in some sense, owing to model uncertainties, its trajectories could display very poor convergence performance and/or exhibit an oscillating behavior. Therefore, combining it with the RC unit dynamics, ensuring stabilization could require complex dynamic compensators for the repetitive update law: this is in contrast to the target of an easy-to-tune RC unit.

Considering the steady-state condition, we assume that a small enough  $T$ -periodic action by the RC unit (a sort of open-loop action of the RC) makes the system given by the plant and the disturbance observer converge to a  $T$ -periodic steady state. Even referring to such  $\Omega$ -limit behavior, we can expect an inaccurate disturbance estimate, owing to model uncertainties. The ensuing architecture is therefore proposed. Beside the disturbance observer, following a hybrid approach, a jump dynamics is adopted to periodically update the overall state of the repetitive unit. The jump period  $T_H$  is selected so that  $T_H \gg T$  and to be enough large to ensure that, when a jump takes place, the drive controller, the plant and the disturbance observer are very close to the steady-state corresponding to the correction applied at the previous jump. This “modify and wait” approach makes the control scheme much less sensitive to the dynamic inaccuracy of the disturbance estimator<sup>4</sup>. Still, steady-state inaccuracy has to be managed by the jump dynamics.

In the following paragraphs we describe the design of this part, deriving formal convergence and robustness properties against steady-state reconstruction inaccuracies. Then, we present a possible approach for disturbance observer showing how, for the considered case of study, under significant parametric uncertainties, the steady-state inaccuracies comply with the robustness domain of the proposed hybrid update law.

### 3.1.1 Jump dynamics for repetitive unit update

As shown in Fig. 4, a  $T_H$ -periodic jump is introduced to update at the same time the full state of the repetitive unit, vector  $\chi$ . To this purpose, the disturbance observer has been enriched with a delay line to expose to the update unit a full  $T$ -period of the disturbance estimation. This disturbance, vector  $\hat{d}_s$ , is shifted by the delay  $m$  to take into account the known delay affecting the reconstruction. The obtained shifted vector,  $\hat{d}$ , is then used to update the repetitive unit. It is worth noting that, defining  $\hat{d}_T$  as the vector collecting the  $N$  (shifted) samples of  $d_T$ , vector  $\hat{d}$  is not the reconstruction of  $\hat{d}_T$ , but the estimation of the difference between  $\tau_R$ , seen over one  $T$ -period, and the disturbance  $\hat{d}_T$ .

Therefore, we can employ  $\hat{d}$  for the correction of the RC unit

through a simple proportional law ( $-K\hat{d}$ ) in a “one step full update” approach. Notice that this shifting and updating mechanism is equivalent to feeding by elements of vector  $-K\hat{d}$  the repetitive unit structure proposed in Fig. 3.

To analyze the properties of the proposed update mechanism, the relation between  $\chi$ ,  $\hat{d}_T$  and  $\hat{d}_s$  (or equivalently  $\hat{d}$ ) is crucial. As said,  $\chi$  is updated every  $T_H$  and such time is selected to be very large w.r.t. the convergence dynamics of the system composed by the regulator, the plant and the disturbance observer.

For this reason, it is possible to assume that, at each jump,  $\hat{d}_s$  is very close to the steady-state of such system driven by  $\chi$  (imposed in the previous jump) and  $\hat{d}_T$ .

In particular, defining  $\tilde{\chi} := \chi - \hat{d}_T \in \mathbb{R}^N$  we can introduce

<sup>4</sup> In addition, it paves the way to the delay adaptation, which is addressed later on.

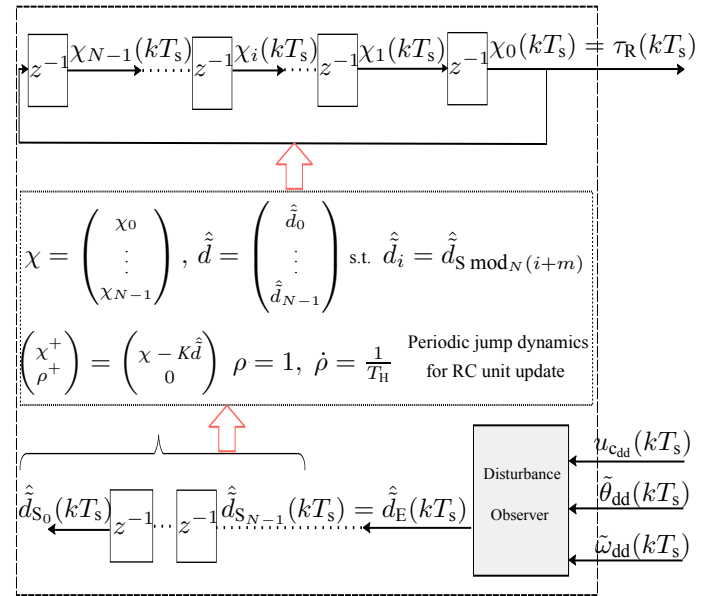


Fig. 4. Scheme of the proposed RC unit embedded in the motion controller as shown in Fig. 2.

a map  $H : \mathbb{R}^N \rightarrow \mathbb{R}^N$  such that, for all  $\tilde{\chi}$ ,  $H(\tilde{\chi})$  represents the steady-state behavior of  $\hat{d}$ , and we can assume  $\hat{d} \simeq H(\tilde{\chi})$  in the jump dynamics analysis, introducing a reduced order hybrid system. Then, we can define the following error dynamics related to the original system in Fig. 4:

$$\mathcal{H}_{\tilde{\chi}} : \begin{cases} \begin{pmatrix} \dot{\tilde{\chi}} \\ \dot{\rho} \end{pmatrix} = \begin{pmatrix} 0_{N \times 1} \\ \Lambda \end{pmatrix}, & \begin{pmatrix} \tilde{\chi} \\ \rho \end{pmatrix} \in C_{\tilde{\chi}} \\ \begin{pmatrix} \tilde{\chi}^+ \\ \rho^+ \end{pmatrix} = \begin{pmatrix} \tilde{\chi} - KH(\tilde{\chi}) \\ 0 \end{pmatrix}, & \begin{pmatrix} \tilde{\chi} \\ \rho \end{pmatrix} \in D_{\tilde{\chi}} \end{cases} \quad (6)$$

with positive scalars  $K$  and  $\Lambda = 1/T_H$ ,  $C_{\tilde{\chi}} = \mathbb{R}^N \times [0, 1]$  and  $D_{\tilde{\chi}} = \mathbb{R}^N \times \{1\}$ . For compactness of notation, let  $q(\tilde{\chi}) = \tilde{\chi} - KH(\tilde{\chi})$ .

Clearly, for a perfect disturbance observer with no steady-state mismatches,  $H(\cdot)$  would be the identity map. In the following we introduce some assumptions on  $H(\cdot)$  to represent a meaningful class of possible inaccuracies, then we show that the proposed simple update law guarantees a correct convergence, despite such deviations.

**Assumption 1.** The map  $H(\cdot) : \mathbb{R}^N \rightarrow \mathbb{R}^N$  is continuous in  $\mathbb{R}^N$  and such that:

- $H(\tilde{\chi}) = 0$  if and only if  $\tilde{\chi} = 0$ ;
- there exists a positive scalar  $K^*$  such that,  $\forall \tilde{\chi} \in \mathbb{R}^N$ , it holds:

$$\tilde{\chi}^T H(\tilde{\chi}) - \frac{K^*}{2} H^T(\tilde{\chi}) H(\tilde{\chi}) \geq 0. \quad (7)$$

**Assumption 2.**  $H(\cdot)$  is differentiable in the origin. Furthermore, there exist a symmetric positive definite matrix  $P$  and a positive scalar  $b$  such that:

$$\left( \frac{\partial H}{\partial \tilde{\chi}}(0) \right)^T P \left( \frac{\partial H}{\partial \tilde{\chi}}(0) \right) \geq bI_N. \quad (8)$$

The above assumptions represent respectively:

- (1) an enriched passivity request for the static map  $H(\cdot)$ , similar to the conditions in (Arimoto and Naniwa, 2000);

(2) a requirement for a linear behavior in the origin and close to it.

In the next statements, let  $\phi(t, j) = (\phi_{\tilde{x}}, \phi_{\rho})(t, j)$  indicate the solutions of system  $\mathcal{H}_{\tilde{x}}$  at time  $(t, j)$ . Additionally, let the sequence of positive scalars  $0 = t_0 \leq t_1 < \dots < t_j \leq t_{j+1} = t$  be such that:

$$\text{dom } \phi \cap ([0, t] \times \{0, \dots, j\}) = \bigcup_{i=0}^j [t_i, t_{i+1}] \times \{i\}. \quad (9)$$

It can be easily checked that system  $\mathcal{H}_{\tilde{x}}$  verifies a reverse average dwell-time: this fact is used to establish the following stability result.

**Proposition 1.** Consider system  $\mathcal{H}_{\tilde{x}}$  and let Assumption 1 hold. Pick, and fix, a positive scalar  $K$  satisfying  $0 < K < K^*$ . Then, the attractor  $\mathcal{A}_0 := 0_{N \times 1} \times [0, 1]$  is uniformly globally pre-asymptotically stable. In particular, there exists a class  $\mathcal{KL}$  function  $\beta_s$  such that, for any solution  $\phi$  of system  $\mathcal{H}_{\tilde{x}}$  and all  $(t, j) \in \text{dom } \phi$ , it holds:

$$|\phi_{\tilde{x}}(t, j)| \leq \beta_s(|\phi_{\tilde{x}}(0, 0)|, t + j). \quad (10)$$

**Proof:** Consider the Lyapunov function candidate

$$V(\tilde{x}) = |\tilde{x}|^2, \quad (11)$$

and note that, for any  $(\tilde{x}, \rho) \in D_{\tilde{x}}$ , it holds:

$$\begin{aligned} V(q(\tilde{x})) - V(\tilde{x}) &= (\tilde{x} - KH(\tilde{x}))^T (\tilde{x} - KH(\tilde{x})) - \tilde{x}^T \tilde{x} \\ &= 2K \left[ -\tilde{x}^T H(\tilde{x}) + \frac{K}{2} H^T(\tilde{x}) H(\tilde{x}) \right]. \end{aligned}$$

By adding and subtracting the term  $KK^*H^T(\tilde{x})H(\tilde{x})$  we get:

$$\begin{aligned} V(q(\tilde{x})) - V(\tilde{x}) &= -2K \left[ \tilde{x}^T H(\tilde{x}) - \frac{K^*}{2} H^T(\tilde{x}) H(\tilde{x}) \right] + \\ &\quad - K(K^* - K)H^T(\tilde{x})H(\tilde{x}). \end{aligned}$$

The term in the square brackets is positive because of Assumption 1. So, picking  $0 < c \leq K(K^* - K)$ , we obtain:

$$V(q(\tilde{x})) - V(\tilde{x}) \leq -c|H(\tilde{x})|^2. \quad (12)$$

Since  $|H(\tilde{x})|^2$  is positive definite (see Assumption 1), it follows that (Goebel et al., 2012, Proposition 3.24) can be employed to yield uniform global pre-asymptotic stability of the attractor  $\mathcal{A}_0$ . Finally, the bound (10) is a direct consequence of (Goebel et al., 2012, Theorem 3.24).  $\square$

In case also Assumption 2 holds, it is possible to establish a convergence rate for  $|H(\cdot)|^2$ .

**Proposition 2.** Consider system  $\mathcal{H}_{\tilde{x}}$  and let Assumptions 1, 2 hold. Pick any positive scalar  $R$ . Then, there exists a positive scalar  $\gamma$  and a non-negative scalar  $M$  such that, for any  $|\phi_{\tilde{x}}(0, 0)| \leq R$ , it holds:

$$|H(\phi_{\tilde{x}}(t, j))|^2 \leq e^{(M-\gamma j)} |H(\phi_{\tilde{x}}(0, 0))|^2. \quad (13)$$

**Proof:** Let:

$$W(\tilde{x}) := H^T(\tilde{x})PH(\tilde{x}), \quad (14)$$

and note that

$$\lambda_{\min}(P)|H(\tilde{x})|^2 \leq W(\tilde{x}) \leq \lambda_{\max}(P)|H(\tilde{x})|^2, \quad (15)$$

where  $\lambda_{\min}(\cdot)$ ,  $\lambda_{\max}(\cdot)$  denote the minimum and maximum eigenvalue of the argument. Since both  $W$  and its derivative vanish at the origin, we can expand  $W$  as follows:

$$\begin{aligned} W(\tilde{x}) &= \tilde{x}^T \left( \frac{\partial H}{\partial \tilde{x}}(0) \right)^T P \left( \frac{\partial H}{\partial \tilde{x}}(0) \right) \tilde{x} + \tilde{x}^T \delta(\tilde{x}) \\ &= \tilde{x}^T Q \tilde{x} + \tilde{x}^T \delta(\tilde{x}), \end{aligned} \quad (16)$$

with  $Q$  a positive definite matrix from Assumption 2 and  $\delta(\cdot)$  satisfying:

$$\frac{|\delta(\tilde{x})|}{|\tilde{x}|} \rightarrow 0 \text{ as } \tilde{x} \rightarrow 0. \quad (17)$$

From this property, it follows that there exists a positive scalar  $r$  such that, for all  $|\tilde{x}| \leq r$ , it holds  $|\delta(\tilde{x})| \leq b/2|\tilde{x}|$ . Hence we have, for all  $|\tilde{x}| \leq r$ :

$$W(\tilde{x}) \geq \tilde{x}^T Q \tilde{x} - |\tilde{x}||\delta(\tilde{x})| \geq \tilde{x}^T Q \tilde{x} - \frac{b}{2}|\tilde{x}|^2, \quad (18)$$

which exploiting Assumption 2 becomes:

$$W(\tilde{x}) \geq \frac{b}{2}|\tilde{x}|^2. \quad (19)$$

On the other hand, from Proposition 1 we establish the following chain:

$$V(\tilde{x}) \geq V(\tilde{x}) - V(q(\tilde{x})) \geq c|H(\tilde{x})|^2. \quad (20)$$

Combining the latter with the upper bound of  $W$  provided by (15), it is possible to find a positive scalar  $c_2$  such that:

$$W(\tilde{x}) \leq c_2 V(\tilde{x}). \quad (21)$$

Therefore, from (19) and (21), we can claim that there exist positive scalars  $c_1, c_2$  (with  $c_1$  depending on  $R$ ) such that, for all  $|\tilde{x}| \leq R$ , it holds:

$$c_1 V(\tilde{x}) \leq W(\tilde{x}) \leq c_2 V(\tilde{x}). \quad (22)$$

Considering the result of (12) and recalling that  $W(\tilde{x}) \leq \lambda_{\max}(P)|H(\tilde{x})|^2$ , it follows that:

$$V(q(\tilde{x})) - V(\tilde{x}) \leq -\frac{c}{\lambda_{\max}(P)}W(\tilde{x}). \quad (23)$$

Exploiting the lower bound of  $W$  reported in (22), it is possible then to imply the existence of a positive scalar  $\gamma$  satisfying:

$$V(q(\tilde{x})) - V(\tilde{x}) \leq -(1 - e^{-\gamma})V(\tilde{x}), \quad (24)$$

which in turn means that, for  $i \in \{1, \dots, j\}$ :

$$|\phi_{\tilde{x}}(t_i, i)|^2 \leq e^{-\gamma} |\phi_{\tilde{x}}(t_i, i-1)|^2, \quad (25)$$

hence:

$$|\phi_{\tilde{x}}(t, j)|^2 \leq e^{-\gamma j} |\phi_{\tilde{x}}(0, 0)|^2. \quad (26)$$

Recalling the bounds on  $W$ , given both by (15) and by (22), we can finally write:

$$\begin{aligned} |H(\phi_{\tilde{x}}(t, j))|^2 &\leq \frac{c_2}{\lambda_{\min}(P)} |\phi_{\tilde{x}}(t, j)|^2 \\ &\leq \frac{c_2 \lambda_{\max}(P)}{c_1 \lambda_{\min}(P)} e^{-\gamma j} |H(\phi_{\tilde{x}}(0, 0))|^2, \end{aligned} \quad (27)$$

which yields the bound of the statement after selecting  $M = \log((c_2 \lambda_{\max}(P))/(c_1 \lambda_{\min}(P))) \geq 0$ .  $\square$

### 3.1.2 Disturbance observer for the considered 1 DOF Lagrangian system

We propose to develop the disturbance observer by considering the linearized plant dynamics around the assigned trajectory  $\bar{\theta}^*(t), \bar{\omega}^*(t), \bar{\tau}^*(t)$ . Assuming the initial conditions  $\bar{\theta}(t_0), \bar{\omega}(t_0)$  and  $\bar{\tau}, d, \bar{u}$  to be sufficiently small, we can linearly approximate system (4) as follows:

$$\begin{aligned} \begin{pmatrix} \dot{\hat{\theta}}(t) \\ \dot{\hat{\omega}}(t) \end{pmatrix} &= A(t) \begin{pmatrix} \hat{\theta}(t) \\ \hat{\omega}(t) \end{pmatrix} + B(t)(d(t) - \bar{\tau}(t) + \\ &\quad + \bar{u}(t) + \bar{\tau}_{\text{Rd}}(t)), \end{aligned} \quad (28)$$

where  $A(t)$ ,  $B(t)$  are computed from the differentiation of system (4) around  $\bar{\theta}^*(t)$ ,  $\bar{\omega}^*(t)$ ,  $\bar{\tau}^*$ , while  $\bar{\tau}_{\text{Rd}}$  is given as follows:

$$\bar{\tau}_{\text{Rd}}(t) = \tau_{\text{Rd}} \left( \left( \text{floor} \left( \frac{t}{T_s} \right) - 1 \right) T_s \right)$$

The approximated discrete-time linearized model is defined as:

$$\begin{aligned} \tilde{x}((k+1)T_s) &= A_d(kT_s)\tilde{x}(kT_s) + B_d(kT_s)[u_c((k-1)T_s) \\ &\quad + \tau_{\text{Rd}}((k-1)T_s) - d_T(kT_s)] \end{aligned} \quad (29)$$

where  $\tilde{x}(kT_s) = (\tilde{\theta}(kT_s) \tilde{\omega}(T_s))^T$ , while  $A_d$ ,  $B_d$  are computed as:

$$A_d(kT_s) = e^{A(kT_s)T_s}, \quad B_d(kT_s) = \int_0^{T_s} e^{A(kT_s)(T_s-\tau)} B(kT_s) d\tau. \quad (30)$$

Clearly, the above discretization is not exact, since the state evolution matrix is approximated by the matrix exponential adopted for linear time-invariant systems. In this respect, it is worth to recall that our target is not to achieve a perfect disturbance reconstruction, but an estimation whose inaccuracies comply with the robustness properties of the proposed jump dynamics.

To arrange the disturbance observer exploiting (29), we need to consider the delay in reading  $\tilde{\theta}(kT_s)$ ,  $\tilde{\omega}(kT_s)$ ,  $u_c(kT_s)$  and in actuating  $\tau_{\text{R}}(kT_s)$ . Let  $\tilde{x}_{\text{dd}}(kT_s) = (\tilde{\theta}_{\text{dd}}(kT_s) \tilde{\omega}_{\text{dd}}(kT_s))^T$  and let  $B_d^\dagger(\cdot)$  be the pseudoinverse of matrix  $B_d(\cdot)$ . By delaying and inverting system (29), the following disturbance observer is proposed:

$$\begin{aligned} \hat{d}_E(kT_s) &= B_d^\dagger((k-p-1)T_s) [\tilde{x}_{\text{dd}}(kT_s) \\ &\quad - A_d((k-p-1)T_s)\tilde{x}_{\text{dd}}((k-1)T_s)] - u_{\text{cad}}((k-2)T_s). \end{aligned} \quad (31)$$

It is worth pointing out that a similar disturbance observer could be constructed by manipulation of only one of the two scalar equations of (29). Here, we defined  $\hat{d}_E(kT_s)$  the estimation of  $\tau_{\text{Rd}}((k-p-2)T_s) - d_T((k-p-1)T_s)$  or equivalently  $\tau_{\text{R}}((k-2p-2)T_s) - d_T((k-p-1)T_s)$ . Note that,  $d_T((k-p-1)T_s)$  can be reinterpreted as  $\hat{d}_T((k-2p-2)T_s)$ , i.e., the signal  $\tau_{\text{R}}$  which is expected to be generated by the repetitive unit at time  $(k-2p-2)T_s$ . Therefore,  $\hat{d}_E(kT_s)$  is an estimation of the error of the correction action generated at time  $(k-2p-2)T_s$  by the repetitive unit. Samples of  $\hat{d}_E(kT_s)$  are collected in the vector  $\hat{\tilde{d}}_s$ , as shown in Fig. 4, for repetitive “memory” updating, after a shifting by the total delay  $m = 2p + 2$ .

The above disturbance observer, besides the delay  $m$ , will be affected by dynamic and steady-state inaccuracies. The former will be managed by selecting a long-enough update interval for the jump dynamics. In particular, for the considered four-bar linkage and its drive controller, a convergence time of 12s can be estimated<sup>5</sup>, therefore we set  $T_H = 20$ s. As far as steady-state inaccuracies are concerned, it is necessary to verify that the proposed observer complies with the robustness capability given by the jump dynamics<sup>6</sup>. To this aim, the structural properties of map  $H(\cdot)$  should be investigated. Since it is

<sup>5</sup> details on how to derive such data, exploiting the range of admissible inaccuracies and intrinsic modelling approximation, are omitted for brevity.

<sup>6</sup> actually the given assumptions on the jump dynamics are sufficient for convergence and not strictly necessary.

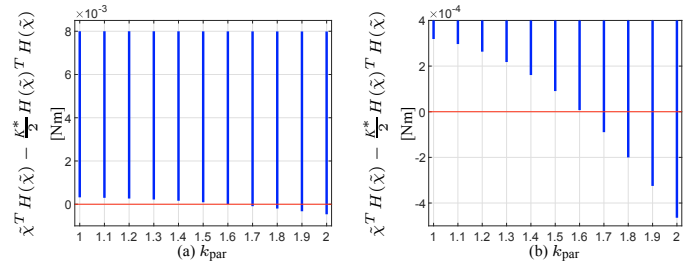


Fig. 5. (a) Left side of condition (7) (with zoom in plot (b)) depending on the model parametric uncertainties.

hard to find an analytical expression for  $H(\cdot)$ , we performed extensive simulation tests by feeding the plant with a known  $T$ -periodic input signal  $\tilde{\chi}$  and by looking at the resulting  $H(\tilde{\chi}) \simeq \hat{d}$ .  $\tilde{\chi}$  has been varied within a limited set of sinusoidal signals with different amplitudes and frequencies of the form:

$$\tilde{\chi}(t)_{(i_d, j_d)} = A_d(i_d) \sin \left( 2\pi f(j_d) \text{floor} \left( \frac{t}{T_s} \right) T_s \right) \quad (32)$$

with

$$\begin{aligned} A_d(i_d) &= \frac{i_d}{5} A_d & i_d &= 1, \dots, 5 \\ f(j_d) &= \begin{cases} 1/T & j_d = 0 \\ \frac{1000 j_d}{T} & j_d = 1, \dots, 5. \end{cases} \end{aligned} \quad (33)$$

The maximum disturbance amplitude  $A_d$  has been fixed to 0.2 Nm, which is a reasonable magnitude for our application as clarified in Section 4. Considering the disturbance periodicity, we have chosen  $T = 2$  s so that, in the worst case given by  $j_d = 0$ ,  $T$  is 10 times smaller than  $T_H$ .

**Passivity-like assumption** To have a fast enough convergence rate for the considered application, we selected  $K^* = 1.2$  (see Subsection 3.2 for further details). We computed the left side of (7) for every  $\tilde{\chi}$  in the aforementioned set, always obtaining positive values. Then, to check validity of condition (7) also in presence of parametric uncertainties, we multiplied both the inertia and the potential energy terms of the plant by  $k_{\text{par}} > 1$ , whereas we kept the parameters used for the disturbance observer equal to the original ones of Fig. 1. As expected, the higher the mismatch between  $H(\tilde{\chi})$  and  $\tilde{\chi}$ , the higher the possibility to violate condition (7). Fig. 5 shows the values of the left side term of (7) for increasing  $k_{\text{par}}$ : for  $k_{\text{par}} < 1.6$  condition (7) is always satisfied.

**$W(\tilde{\chi})$  bounds** Firstly, we set matrix  $P$  of condition (8) equal to the identity, so that  $W(\tilde{\chi}) = |H(\tilde{\chi})|^2$ . Recalling the initial steps made in the proof of Proposition 2, we know that if (8) and Proposition 1 hold, then it is always possible to bound  $W(\tilde{\chi})$  from above and from below, as results in eq. (22) in which  $V(\tilde{\chi}) = |\tilde{\chi}|^2$ . Such condition guarantees an asymptotic convergence of  $|H(\tilde{\chi})|^2$  and the same for the norm of  $\hat{d}$ , whether the overall delay  $mT_s$  is properly compensated.

Fig. 6 shows the values of  $|H(\tilde{\chi})|^2$  for the different  $\tilde{\chi}$  within the considered set. We repeated the tests with and without uncertainties in the model parameters ( $k_{\text{par}} = 1$  and  $k_{\text{par}} = 1.6$ ). It is evident that, for an almost ideal disturbance observer it holds  $H(\tilde{\chi}) \simeq \tilde{\chi}$ , and so  $|H(\tilde{\chi})|^2 \simeq |\tilde{\chi}|^2$  (see Fig. 6(a)). Indeed, in the case of parametric uncertainties, the value of  $|H(\tilde{\chi})|^2$  does not depend only on  $|\tilde{\chi}|$ , but also on the harmonic content of such disturbance. However this is not an issue as long as

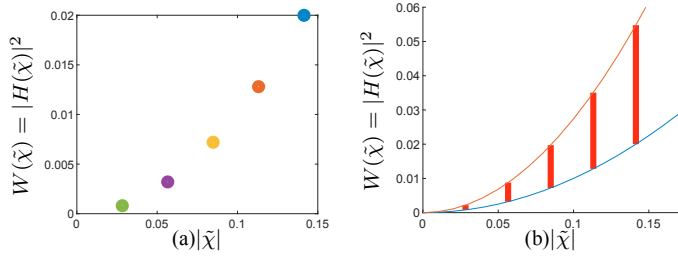


Fig. 6.  $W(\tilde{x})$  behavior (a) without parametric uncertainty, (b) with parametric uncertainty ( $k_{\text{par}} = 1.6$ ).

$|H(\tilde{x})|^2$  remains bounded within  $c_1V(\tilde{x})$  and  $c_2V(\tilde{x})$ . So, the fundamental point is to find some proper values for  $c_1$  and  $c_2$  so that condition (22) holds. We have computed such values considering the worst case scenario, with  $k_{\text{par}} = 1.6$ , so that the resulting bounds remain valid for any  $1 \leq k_{\text{par}} < 1.6$ . Exploiting the data of Fig. 6(b), we have obtained the following values of  $c_1$  and  $c_2$ :  $c_1 = 0.9997$  and  $c_2 = 2.7401$ .

*Remark 2.* As anticipated in the Introduction, the plant, drive control, and disturbance observer dynamics are regarded as flows w.r.t. the jumps dynamics for the RC updates, even if the drive controller and the observer are implemented as discrete-time systems. This is motivated by the fact that the sampling time  $T_s$ , used for discretization of their dynamics, is much smaller than  $T_H$  used for the periodic correction of the repetitive unit.

*Remark 3.* A time-scale separation has been enforced to decouple the flow and jump dynamics. A complete stability analysis would require a deeper study of the disturbance observer. In addition, singular perturbation arguments could be exploited to analyze the overall closed-loop system resulting from the interconnection of the two time-scales subsystems. This part is not addressed here for brevity.

### 3.2 Unknown delay case

In this Subsection we assume that the communication delay  $p$  is unknown, and, in turn, so is the total delay  $m = 2p + 2$  adopted to shift the disturbance vector in the jump dynamics reported in Figure 4. The purpose is then to define an estimate of  $p$ , denoted as  $\hat{p}$ , with a suitable adaptation law to be joined to the hybrid control structure described in Subsection 3.1 (following a sort of certainty equivalence principle). In this regard observe that, assuming  $\hat{p} = p$ , from (13) in Proposition 2 it follows:

$$\bar{J} = \text{floor}\left(\frac{M}{\gamma}\right) + 1$$

$$|H(\tilde{x})(i+l)|^2 \leq e^{(M-\gamma\bar{J})} |H(\tilde{x}(i))|^2 \quad \forall i, \forall l \geq \bar{J}$$

where  $H(\tilde{x})(i) \simeq \hat{d}(i)$  indicates the vector collecting a  $T$ -period generated by the disturbance observer at the  $i^{\text{th}}$  jump. Then, under correct estimation of  $p$ , a contraction of the norm of the residual disturbance reconstruction by  $e^{(M-\gamma\bar{J})} = e^{(\text{mod}_\gamma(M)-\gamma)} < 1$  is expected every  $\bar{J}$  jumps. On the other hand, with an incorrect estimate, no guarantees can be given. In this case, it is reasonable that  $|H(\tilde{x})|^2$  decreases with a smaller contraction ratio or even it increases “sooner or later”.

From these considerations, the following jump dynamics is formulated to update  $\hat{p}$  and to be combined with the structure reported in Fig. 4.

$$\left\{ \begin{array}{l} \begin{pmatrix} \dot{\eta} \\ \dot{\mu} \\ \dot{\hat{p}} \\ \dot{\rho} \end{pmatrix} = \begin{pmatrix} 0 \\ 0 \\ 0 \\ \Lambda \end{pmatrix} \\ \eta^+ = \begin{cases} \eta + 1 & \text{if } \eta + 1 < \bar{J} \\ 0 & \text{if } \eta + 1 = \bar{J} \end{cases} \\ \mu^+ = \begin{cases} \mu & \text{if } \eta + 1 < \bar{J} \\ |\hat{d}| & \text{if } \eta + 1 = \bar{J} \end{cases} \\ \hat{p}^+ = \begin{cases} \hat{p} & \text{if } \eta + 1 < \bar{J} \\ \hat{p} & \text{if } \eta + 1 = \bar{J} \ \& \ |\hat{d}| \leq \mu e^{(\text{mod}_\gamma(M)-\gamma)} \\ \hat{p} + 1 & \text{if } \eta + 1 = \bar{J} \ \& \ |\hat{d}| > \mu e^{(\text{mod}_\gamma(M)-\gamma)} \end{cases} \\ \rho^+ = 0 \end{array} \right. \begin{cases} \begin{pmatrix} \eta \\ \mu \\ \hat{p} \\ \rho \end{pmatrix} \in \hat{C} \\ \begin{pmatrix} \eta \\ \mu \\ \hat{p} \\ \rho \end{pmatrix} \in \hat{D} \end{cases} \quad (34)$$

with  $\hat{C} = \mathbb{N} \times \mathbb{R} \times \mathbb{N} \times [0, 1]$ ,  $\hat{D} = \mathbb{N} \times \mathbb{R} \times \mathbb{N} \times \{1\}$ , and  $\rho$  having the same dynamics as in (6), so  $\Lambda = 1/T_H$ . The initial conditions can be set to  $\eta(t_0, 0) = 0$ ,  $\hat{p}(t_0, 0) = 0$ , and  $\mu(t_0, 0) = +\infty$  (i.e. a very large value to avoid inappropriate update of  $\hat{p}$  at the first jump). The overall delay estimate is given by  $\hat{m} = 2\hat{p} + 2$ .

The adaptation law reported above can be interpreted as follows. Starting with  $\hat{p} = 0$ , whenever the contraction condition on  $|\hat{d}|^2 \simeq |H(\tilde{x})|^2$  is met, the delay estimation is not updated. As soon as a not sufficient decrease or an increase is detected,  $\hat{p}$  is augmented by one. Detailed analysis of the convergence properties of such mechanism is not reported for brevity. We just remark that, in the unlikely case a persistent decrease of  $|H(\tilde{x})|^2$  by  $e^{(\text{mod}_\gamma(M)-\gamma)}$  was obtained even with a wrong estimate of  $p$ , then  $|H(\tilde{x})|^2$  would asymptotically reach zero as the number of jumps goes to infinity. This would give, in turn, a vanishing  $|\tilde{x}|^2$  and the control objective of Section 2 would be achieved.

Referring to the considered four-bar linkage, we determined values for  $M$ ,  $\gamma$ , and then  $\bar{J}$ . For what concerns  $M$ , recalling its definition that stems from (27) and that  $P = I$ , it follows:

$$M = \log \frac{c_2}{c_1} = 1.0083.$$

Then, parameter  $\gamma$  is determined in the following way:

- Combining (12) and (22), and recalling that  $W(\tilde{x}) = |H(\tilde{x})|^2$ , yields:

$$V(q(\tilde{x})) - V(\tilde{x}) \leq -c c_1 V(\tilde{x}) \quad (35)$$

- Having selected  $K^* = 1.2$ , we set  $K$  to 0.6, and parameter  $c$  to  $K(K^* - K)$  so that (12) holds true.
- Then, from eq. (24) and (35) it follows

$$1 - e^{-\gamma} = c c_1 \rightarrow \gamma = -\log(1 - c c_1) = 0.4461.$$

Finally, we obtain  $\bar{J} = \text{floor}\left(\frac{M}{\gamma}\right) + 1 = 3$ .

## 4. SIMULATION RESULTS

The proposed repetitive-based control scheme has been tested through simulations. The sampling time  $T_s$  and drive controller parameters are the ones reported in Section 2. For the torque actuation we considered a direct-drive electrical machine (*Robo Drive ILM 85 x 26*) having the following ratings: 2.6 Nm as RMS torque and 8.3 Nm as peak torque. The chosen reference

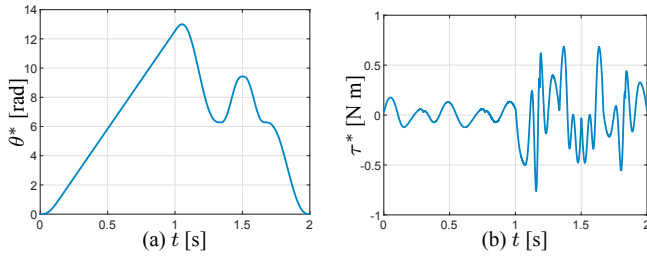


Fig. 7. (a)  $\theta^*$  over one  $T$ -period. (b)  $\tau^*$  over one  $T$ -period.

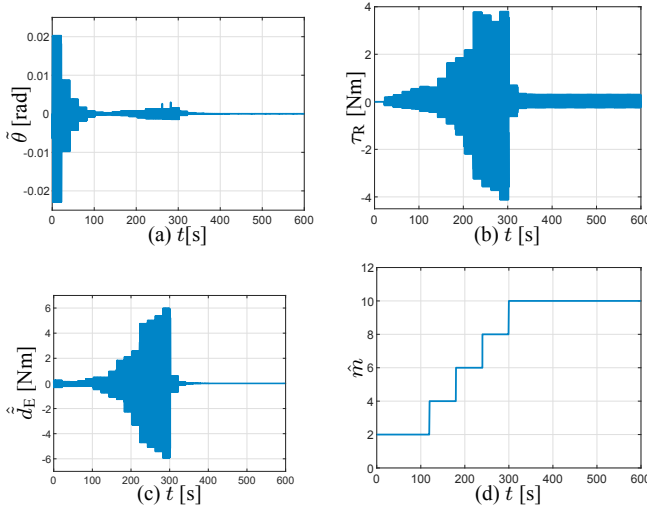


Fig. 8. (a) Position tracking error. (b) Repetitive control action. (c) Reconstructed disturbance. (d) Estimated overall delay.

trajectory is represented in Fig. 7(a), whereas Fig. 7(b) shows the evolution of the corresponding  $\tau^*$  over one  $T$ -period. A transmission delay of  $4T_s$  (i.e.  $p = 4$ ) has been emulated and the model parameters have been increased by 40% w.r.t. the nominal ones of Fig. 1, which are adopted in the overall control unit. An additional torque disturbance  $d$  has been introduced, which has been generated as follows: an amplitude equal to 0.2 Nm (corresponding to 25% of the amplitude of  $\tau^*$ ) and an harmonic content equal to three frequencies ( $1/T$ ,  $4/T$ ,  $1000/T$ ). The obtained results are reported in Fig. 8. As can be noted in Fig. 8(a), the tracking error, that without RC unit would be around 0.2 rad, is reduced to a final bound of  $5 \times 10^{-6}$  rad. A further reduction to zero does not occur because in this case  $d$  does not comply with the matching condition reported in Remark 1. As concerns the delay adaptation, we can notice from Fig. 8(d) that  $\hat{m}$  reaches  $m$  and consequently contraction of  $|\hat{d}|$  is achieved (see Fig. 8(c)). Note also that during the delay adaptation phase reduction of  $|\hat{d}|$  can temporary occur (for instance during the first 50 s of Fig. 8(c)). However after a while, if  $\hat{m} \neq m$  an increase of  $|\hat{d}|$  takes place, so that a delay estimate update is triggered.

## 5. CONCLUSIONS AND FUTURE WORKS

A repetitive control solution for a class of 1-DOF Lagrangian systems has been proposed, showing its effectiveness on a realistic benchmark case. The scheme can be profitably implemented on standard technological architectures adopted for motion control tasks, as an outer repetitive loop can be included without a deep knowledge of the inner controller. Only some technical assumptions on stability of such controller (without

the proposed RC unit) are needed, along with some inaccurate knowledge about the mechanical model. Moreover, the presented strategy can cope with unknown transmission delay, recovering its value in an adaptive fashion. The key elements to achieve such results are a disturbance observer, which approximates the signal to be learned by the RC, and a hybrid strategy to correct the repetitive action when the underlying systems have reached a quasi steady-state condition. Future efforts will be devoted to a deeper analysis of the stability and robustness properties of the overall feedback scheme, and to generalize the approach to a broader class of systems.

## REFERENCES

- Ahn, H.S., Chen, Y., and Moore, K.L. (2007). Iterative learning control: Brief survey and categorization. *IEEE Transactions on Systems, Man, and Cybernetics, Part C (Applications and Reviews)*, 37(6), 1099–1121.
- Arimoto, S. and Naniwa, T. (2000). Equivalence relations between learnability, output-dissipativity and strict positive realness. *International Journal of Control*, 73(10), 824–831.
- Goebel, R., Sanfelice, R.G., and Teel, A.R. (2012). *Hybrid dynamical systems: modeling stability, and robustness*. Princeton University Press, Princeton, NJ.
- Gurocak, H. (2015). *Industrial motion control: motor selection, drives, controller tuning, applications*. John Wiley & Sons.
- Królikowski, A. and Baczyński, P. (2000). Discrete-time repetitive control for plants with time delay. *IFAC Proceedings Volumes*, 33(23), 259–262.
- Liu, T. and Gao, F. (2010). Robust two-dimensional iterative learning control for batch processes with state delay and time-varying uncertainties. *Chemical Engineering Science*, 65(23), 6134–6144.
- Longman, R.W. (2000). Iterative learning control and repetitive control for engineering practice. *International journal of control*, 73(10), 930–954.
- Na, J., Costa-Castelló, R., Griño, R., and Ren, X. (2012). Discrete-time repetitive controller for time-delay systems with disturbance observer. *Asian Journal of Control*, 14(5), 1340–1354.
- Tan, K.K., Zhao, S., Huang, S., Lee, T.H., and Tay, A. (2009). A new repetitive control for lti systems with input delay. *Journal of process Control*, 19(4), 711–716.
- Wang, Y., Gao, F., and Doyle III, F.J. (2009). Survey on iterative learning control, repetitive control, and run-to-run control. *Journal of Process Control*, 19(10), 1589–1600.
- Watanabe, K. and Yamada, K. (1990). Repetitive control of time-delay systems. In *29th IEEE Conference on Decision and Control*, 1685–1690. IEEE.
- Xu, J.X. and Yan, R. (2006). On repetitive learning control for periodic tracking tasks. *IEEE Transactions on Automatic Control*, 51(11), 1842–1848.
- Yu, P., Wu, M., She, J., Liu, K.Z., and Nakanishi, Y. (2017). An improved equivalent-input-disturbance approach for repetitive control system with state delay and disturbance. *IEEE Transactions on Industrial Electronics*, 65(1), 521–531.